A peer-reviewed open-access journal indexed in NepJol
ISSN 2990-7640 (online); ISSN 2542-2596 (print)
Published by Molung Foundation, Kathmandu, Nepal
Article History: Received on April 8, 2024; Accepted on May 30, 2024
DOI: https://doi.org/10.3126/mef.v14i01.67890

First-principles Calculation of Cumene: Molecular Structure, Electronic Structures, Spectroscopic Analysis, and Thermodynamic Properties

Abhishek Rana Magar, Rabin Ghimire, Bishwo Basnet, Prakash Man Shrestha, Suresh Prasad Gupta, and *Krishna Bahadur Rai
Department of Physics, Patan Multiple Campus, Tribhuvan University, Nepal

Author Note

Abhishek Rana Magar https://orcid.org/0009-0001-4593-5972, Rabin Ghimire https://orcid.org/0009-0002-5428-7361, Bishwo Basnet https://orcid.org/0009-0008-1141-7764, Prakash Man Shrestha https://orcid.org/0000-0002-6014-0123, Dr Suresh Prasad Gupta https://orcid.org/0000-0001-9075-468X and Krishna Bahadur Rai https://orcid.org/0000-0001-8882-0385 are currently working at Patan Multiple Campus, Tribhuvan University, Nepal.

We have no known conflict of interest to disclose.

*Correspondence concerning this article should be addressed to Krishna Bahadur Rai, Department of Physics, Patan Multiple Campus, Tribhuvan University, Nepal. Email: krishnarai135@gmail.com

Abstract

This study uses the DFT method for the investigation of optimized structure, electronic structures, charge analysis, FT-IR, FT-Raman spectroscopic analysis and thermodynamic properties. The optimized energy and dipole moment are -9531.775 eV and 0.3818 Debye. The bond lengths of C1-C2 and C1-H7 molecules inside the benzene ring are observed to be 1.39 Å and 1.08 Å respectively. The bond angle of C1-C2-C3 and C2-C1-C6 are found to be 120.10 Å and 119.36 Å. The HOMO-LUMO energy gap is 6.331 eV which corresponds very close to the energy gap of 6.321 eV obtained from density of states. The global parameters with ionization energy value 6.747 eV, electron affinity with 0.4152 eV, chemical potential with -3.5811 eV, electronegativity with 3.5811 eV, global hardness with 3.1659 eV, softness with 0.3148 eV^{-1} and electrophilicity index with 2.0253 eV are obtained. The Mulliken charges analysis indicate that most of the carbon atoms except C4 and C12 are found to carry negative charges where all of the H-atoms are found having positive charge. The molecular electrostatic potential, electrostatic potential and electron density identify different electrophilic and nucleophilic region and its reactive natures. The FT-IR spectroscopy shows strong C-H vibrations at 3186-3093 cm^{-1}, methyl group vibration at 3091-3078 cm^{-1} and the ring vibrations at 1641-1482 cm^{-1}. The heat capacity at constant volume and at constant pressure, internal energy, enthalpy, entropy increase with increasing temperature. However, Gibb's free energy shows opposite nature providing very important insights according to the change in temperature.

Keywords: density functional theory, density of state, molecular electrostatic potential, IR-spectroscopy, thermodynamic properties

First-principles DFT Study of Cumene: Molecular Structure, Electronic Structures, Spectroscopic Analysis and Thermodynamic Properties

Cumene (C_9H_{12}), also known by its other common name, isopropyl benzene, has an IUPAC name of (Propan-2-yl) benzene. It is a buoyant colourless organic liquid compound that, at room temperature, has a sharp, penetrating, aromatic, and gasoline-like odour that acts as one of its crucial characteristics as an aromatic substance. It is a part of an aromatic family that has an origin structure similar to hydrocarbon families, including toluene (methylbenzene and ethylbenzene) with an alkyl substitution on of the hydrogen inside the benzene ring (Nikfar & Behboudi, 2014). When benzene (Rai et al., 2024) is treated with an unsaturated organic compound such as propylene in the presence of phosphoric acid as a catalyst at 250 degree Celsius (ºC), Cumene is formed. It is an ignitable material that is soluble in alcoholic compounds and other solvents but insoluble in water. It is mostly found in gasoline and crude oil, as well as many plant oils, meals, and items that contain tobacco. Another common name for Cumene is 2-penylpropane, or (1-methylethyl) Benzene. It is widely employed in the catalytic synthesis of acetone and phenol (Ghimire et al., 2023). On the other hand, Cumene was first developed as a catalytic agent for the manufacture of aviation gasoline during World War II (Haun & Kobe, 2002). Cumene which has a benzene ring in its structure, indicates that it has one of the aromatic odours in its properties.

Figure 1

Chemical Structure of Cumene

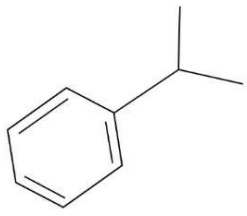

Various studies, research and report have been made till date regarding the study of Cumene molecule. In 2015, Sivaranjani et al., did an investigation on Cumene obtaining FT-IR, FT-Raman, NMR and UV spectra through various spectroscopic techniques. Researchers in 2006 reported the process of Cumene formation through benzene alkylation with propylene on the new three-dimensional catalyst (Jansang et al., 2006). Al-Khattaf & de Lasa (2001) found the process of catalytic cracking of Cumene. Petroselli and colleagues (2017) proposed a report where a new class of lipophilic N-hydroxyphthalimides catalysts, designed for the aromatic oxidation of Cumene in solvent free conditions, were synthesized and tested. Luyben studied the chemical process to form Cumene with the interaction of benzene and propylene and again with the repellent of Cumene with propylene to shape the formation of p-diisopropylbenzene (Luyben, 2010). In 2016 the research of chemical kinetics on thermal decomposition of Cumene hydroperoxide in Cumene by calorimetry was studied where the compound was noted to have a catalytic product reaction (Duh, 2016). Even though the literature review reveals different research regarding the atoms, electrons and overall molecular structure of Cumene, it can be observed that no research for molecular structure, electronic structure, spectroscopic analysis and thermodynamic properties have been performed using the B3LYP/6-311++G(d,p) basis set. So, our objectives are to investigate the optimization energy and its steps, bond length, bond angle, dihedral angle, highest occupied molecular orbitals and lowest unoccupied molecular orbital (HOMO-LUMO), density of states (DOS), global reactivity parameters, Mulliken charges, molecular electrostatic potential (MEP), electrostatic potential (ESP), electron density (ED), vibrational behaviour and thermodynamic parameters of Cumene using the B3LYP/6-311++G(d,p) basis set, filling the research gap identified in the literature review regarding the calculation and analysis of these properties.

Methodology: Computational Details

The overall process for the calculation of different quantum chemical behaviours has been carried out using the Gaussian 09W and GaussView 6.0 version as the primary software for the overall calculations. The geometrical and optimization calculations for the compound Cumene were carried out using the Density Functional Theory (DFT) method with B3LYP/6-311++G(d,p) basis set. Furthermore, the electronic properties such as HOMO-LUMO, MEP, ESP, ED and the vibrational spectroscopy (FT-IR and FT-Raman) were also performed using a similar DFT method and basis set and they had been scaled accordingly. GaussSum 3.0 software package was used as secondary software to generate DOS spectrum related to the calculations. The thermodynamic properties were also been carried out using the same B3LYP/6-311++G (d,p) basis set in the Gaussian software together with the Moltran software. Origin Pro 9.0 had been used as other software for further plotting of different graphs.

Results and Discussion

Optimized Energy and Optimization Steps

The optimization energy of any molecule can be defined as the required energy for any molecule or compound to be in its most stable state. Optimizing step is the process to reduce the energy of the molecule to its minimum state so that it can be stable. Figure 2 shows the steps that were required to reduce the energy of the Cumene molecule and to make it stable, which has an overall total of 3 optimization steps. The maximum energy contained in Hartree has been converted into eV using the conversion value where 1 Hartree = 27.211 eV. Therefore, the molecule was at -9531.7828 eV at step 1, during which the molecule had its highest energy. While coming towards step number 2, the energy has started to decrease with the energy at this step being -9531.7863 eV. Finally, at step number 3, the energy of the molecule has been reduced to its lowest possible energy state, has been neutralized, and has remained stable at this point

with an energy of -9531.7864 eV as shown in Figure 2. Similarly, the dipole moment obtained was measured at 0.3818 Debye.

Figure 2

Energy and Optimization Steps of Cumene Molecule

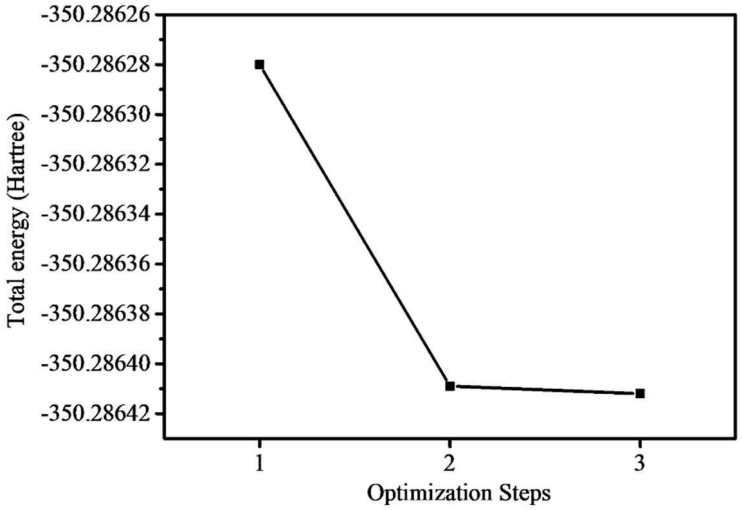

Figure 3

Optimized Structure of Cumene With Symbol and Numbering of Atoms

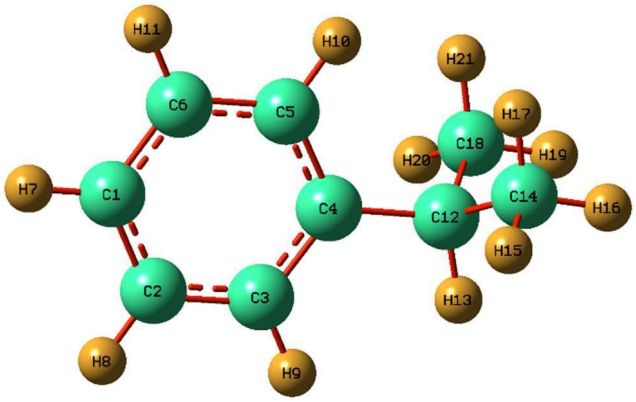

Figure 3 shows the visual representation of optimized structure of the Cumene molecule with different geometrical parameter. It displays the benzene ring formation with the substitution of the methyl group in one of the H-atom,

representing the unique structure of Cumene along with its bond formation of every neighbouring atoms.

Optimization of Molecular Parameters

Table 1 represents the different geometrical parameters of the Cumene molecule. It is observed that the bond length between the carbon-carbon atoms, such as C1-C2, C5-C6 and C2-C3 found to be around 1.392 Å, 1.394 Å, 1.394 Å which agrees approximately with the experimental value of 1.396 ± 0.001. Similarly, the bond length of C1-H7, C5-H10 and C3-H9 atoms are observed to be 1.084 Å, 1.084 Å and 1.085 Å, as shown in Table 1. The bond length between the substituent parts of the molecule can also be observed from Table 1, which corresponds with the experimental values (Weast, 1975). Moreover, the bond angle between the C1-C2-C3, C2-C1-C6, C6-C1-H7 and C4-C6-H10 atoms are observed to be 120.10˚, 119.36˚, 120.29˚ and 119.84˚ which matches relatively very close with the experimental value of 120.1˚ ± 1˚. Furthermore, the different dihedral angles of the four atoms inside the molecules have been recorded using a similar method shown in table 1.

Table 1

Optimized Parameters of Cumene Molecule

Bond length	Value (Å)	Bond Angle	Value (˚)	Dihedral Angle	Value (˚)
C1-C2	1.392	C1-C2-C3	120.10	C6-C1-C2-C3	0.00164
C5-C6	1.394	C2-C1-C6	119.36	C3-C4-C5-H6	0.00208
C2-C3	1.394	C6-C1-H7	120.29	C6-C1-C2-H8	-179.99
C3-C4	1.398	C1-C2-H8	120.10	C3-C4-C5-H10	-179.99
C4-C5	1.401	C4-C5-C6	121.06	C1-C6-C5-C4	-0.00066
C1-C6	1.398	C4-C6-H1O	119.84	C1-C6-C5-H10	179.99
C5-C6	1.392	C4-C3-H9	119.25	C6-C5-C4-C12	179.99

C1-H7	1.084	C2-C3-C4	121.23	C5-C4-C12-C18	-62.74
C5-H10	1.084	C4-C12-C14	111.98	C5-C4-C12-C14	62.76
C3-H9	1.085	C4-C12-C18	111.98	H13-C12-C18-H20	60.76
C4-C12	1.522	C14-C12-C18	111.05	H13-C12-C18-H19	-59.44
C12-C18	1.533	H20-C18-H21	107.78	H15-C14-C12-H13	-60.76
C12-C14	1.533	H15-C14-H17	107.78	H13-C12-C14-H17	179.06
C18-H21	1.094	H16-C14-H17	107.68	C4-C3-C2-C1	0.00
C18-H20	1.092	H15-C14-H16	108.19	H19-C18-C12-C14	57.65
C12-H13	1.095				
H16-C14	1.094				
C14-H17	1.094				
C14-H15	1.094				

HOMO-LUMO Analysis

Figure 4 represents the HOMO-LUMO plot. The electrophilic part having tendency to donate an electron represents the HOMO orbitals while the nucleophilic part having tendency to gain or accept an electron are the LUMO orbitals (Kumer et al., 2019). The present analysis concludes by determining the HOMO-LUMO band gap that is an essential analysis for the study of stability and strength between atoms/molecules. From Figure 4, the area that contains the positive charge are represented by the green part while the area with the negative charge is represented by red parts (Prabhu et al., 2023). In Figure 4, HOMO energy is -6.747 eV and LUMO energy is -0.4152 eV such that the energy gap (ΔE) in the ground state level is calculated as 6.331 eV. The HOMO-LUMO gap represents the hardness of the molecule, indicating that the harder the molecule, the more the energy is required to break the bonds in between them. In the case of Cumene, the HOMO-LUMO gap is observed to be quite high, i.e., 6.331 eV,

showcasing that the Cumene molecule has a high chemical hardness. The HOMO-LUMO band gap i.e. 6.81 eV in gas phase calculated using the basis set of 6-31++G (d,p) (Sivaranjani et al., 2015) is comparable to our HOMO-LUMO band gap.

Figure 4

The Atomic Orbital Compositions of the Frontier Molecular Orbital, HOMO-LUMO Energy gap of Cumene

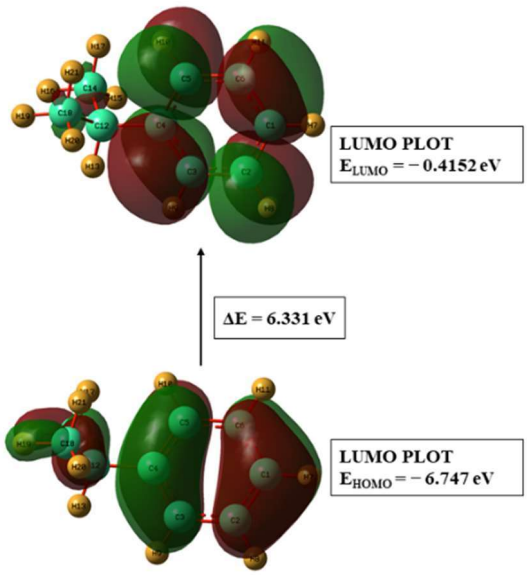

Density of States (DOS)

Figure 5 shows the DOS plot for the Cumene molecule. The density of the state is the area of energy level that is available for an electron. The green part denotes the occupied orbitals having free electrons that can be donated while the red part represents the virtual state, representing the tendency to accept the electron. The energy gap (Dhakal & Rai, 2023; Ghimire et al., 2021) obtained from the DOS plot, i.e. 6.321 eV agrees approximately with the energy gap from the HOMO-LUMO band gap, i.e., 6.331 eV.

Figure 5

Density of State Plot of Cumene Molecule

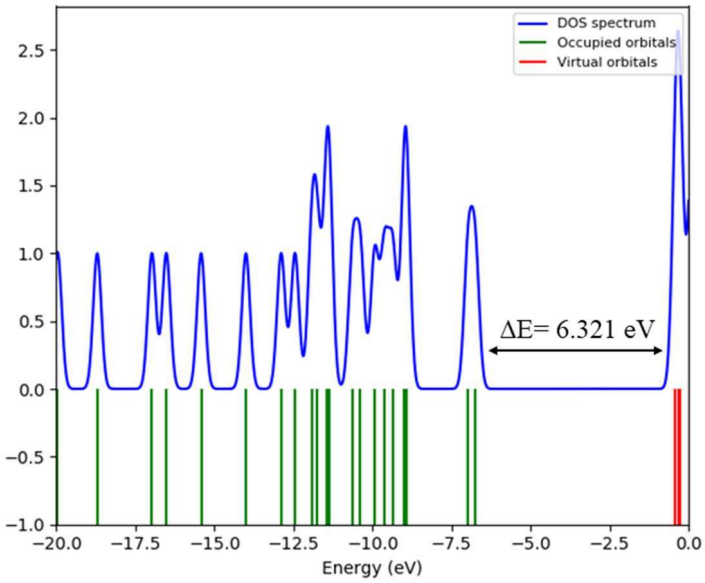

Global Reactivity Parameters Calculation

For the analysis of global reactivity parameters such as ionization potential (I), electron affinity (A), chemical potential (μ), electronegativity (χ), hardness (η), softness (ζ) and electrophilicity index (ω), Koopman's theory states that HOMO and LUMO orbitals are interrelated with the parameters of ionization potential (I) and electron affinity (A), where the negative part from the highest occupied molecular orbital (HOMO) and the negative of the lowest unoccupied molecular orbital (LUMO) correspond with the ionization potential (I) (which loses an electron) and electron affinity (A) (which gains an electron) respectively (Kaya & Kaya, 2015).

$$I = -E_{HOMO} \quad (1)$$

$$A = -E_{LUMO} \quad (2)$$

The following parameters I and A are found to be 6.747 eV and 0.4152 eV respectively where both of the parameters have positive value and is a satisfactory result.

From the above equation, parameter such as chemical potential (μ) and electronegativity (χ) can be analyzed using the equations (3) and (4) (El-Saady et al., 2023).

$$\mu = -(I+A)/2 \quad (3)$$

$$\chi = (I+A)/2 \quad (4)$$

The following value -3.5811 eV represents the chemical potential (μ) of the molecule. The negative value in this case suggests that the molecule in a chemical reaction tends to move from the higher concentration region towards the lower concentration region. This means that in order to move towards the lower concentration region, it needs to release some amount of energy. Therefore, the obtained value suggests that the Cumene molecule tends to release energy in the chemical reaction. Similarly, the electronegativity (χ) has been observed to be 3.5188 eV. This higher and positive value obtained indicates the strong tendency to attract the electrons. Furthermore, we have the global hardness (η) that can be defined as the resistance between the molecule where it can change or deform their lowest or the occupied orbital state which is also called its electronic configuration due to chemical reaction. This parameter can be calculated with the equation (Torrent-Sucarrat et al., 2002).

$$\eta = (I - A)/2 \quad (5)$$

Moreover, the global softness (ζ) is the inverse of the hardness (η) and is given by the equation below.

$$\zeta = 1/\eta \quad (6)$$

The hardness (η) and softness (ζ) parameters have been observed 3.1659 eV and 0.3148 eV^{-1} respectively, where the hardness of the parameter is significantly higher than the softness and it shows that the molecule has a higher chemical hardness.The global electrophilicity index (ω) can be regarded as the tendency of an atom or a molecule to accept an electron in a chemical reaction (Limbu et al., 2024). This index is given by the equation.

$$\omega = \mu^2/2\eta \quad (7)$$

The global electrophilicity index (ω) has been observed with value of 2.0253 eV, the positive value represents that the analysed molecule is more electrophilic in nature and has a higher tendency to accept an electron in its structure.

The global parameters like electronegativity (χ), chemical hardness (η), softness (ζ) and electrophilicity index (ω) calculated as 3.38 eV, 5.35 eV, 0.19 eV^{-1} and 1.07 eV respectively using the basis set 6-31++G(d,p) (Sivaranjani et al., 2015) are in good agreement to our values 3.5188 eV, 3.1659 eV, 0.3148 eV^{-1} and 2.0253 eV respectively.

Mulliken Charges Analysis

The Mulliken charges analysis represents what the charge density of each atom carries in a molecule (Vinodkumar et al., 2023; Rai et al., 2024) geometry. It means that its value depends upon the electron density of a molecule. In this study, we have calculated the Mulliken population analysis for the Cumene molecule. The bar plot from Figure 6 shows that C1, C2, C3, C5, C6, C14, and C18 are inclined towards the negative charge and C14 and C18 have the highest negative charge values among all the carbon atoms. Similarly, C4, H7, H8, H9, H10, H11, C12, H13, H15, H16, H17, H19, H20, and H21 are the atoms with a positive charge, where C4 has the highest positive charge of all the atoms present.

Figure 6

Mulliken Charges Distribution of Atoms in Cumene Molecule

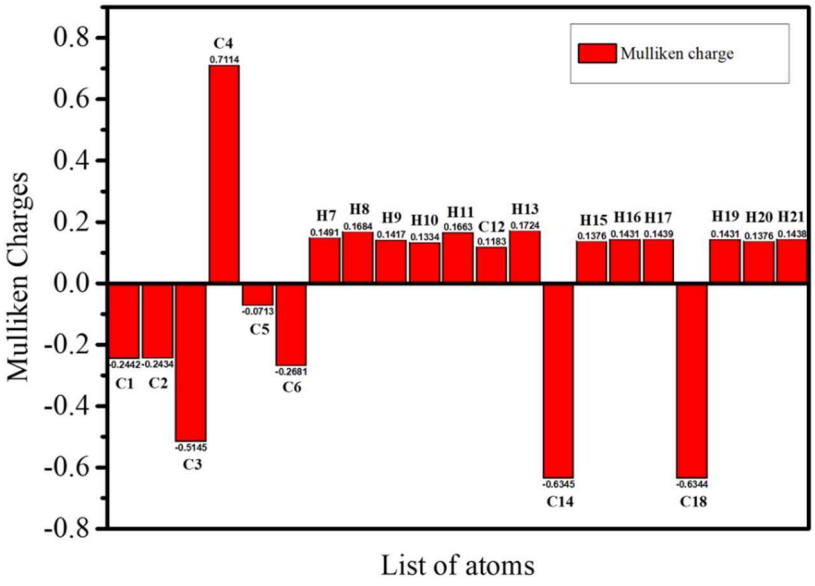

Analysis of Molecular Electrostatic Potential (MEP), Electrostatic Potential (ESP) and Electron Density (ED)

Figures 7(a), 7(b) and 7(c) show the MEP, ESP and ED analysis respectively for the Cumene molecule. MEP which is the electrostatic concentration produced due to the electrophilic (negative) and nucleophilic (positive) attack on the molecule in which the potential of the molecule increases in the following order: red< orange< yellow< green< blue, where red indicates the negative and blue indicates positive with green representing the area where the both attraction and repulsion (neutral) activities are weakest (Ojha et al., 2023). Moreover, potential for the MEP analysis ranges from -2.514e-2 to 2.514e-2 as shown in Figure 7.

Figure 7

(a) Molecular Electrostatic Potential, (b) Electrostatic Potential, (c) Electron Density

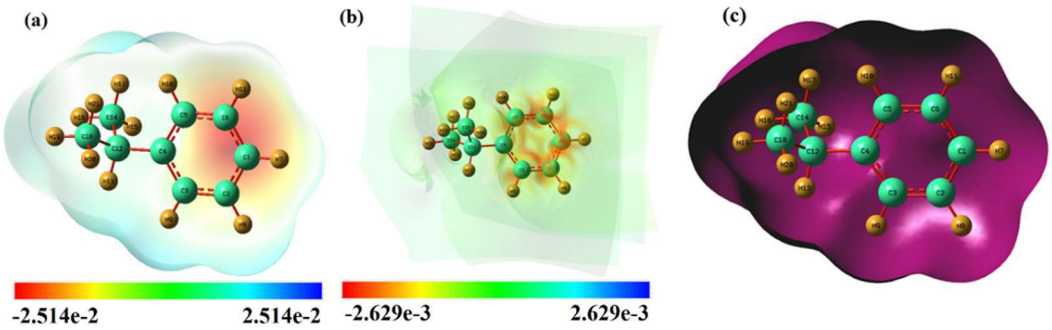

Figure 7(a). The negative region, i.e., the electrophilic (red) region in Figure 7(a), is observed to be concentrated at the centre of the benzene ring symbolizing the region to have the strongest force of attraction and repulsion between the atoms of the molecule. The hydrocarbon group outside of the ring formation i.e. the hydrogen atoms attached to the benzene ring show less electrophilic characteristics (yellow). The green area where the weakest repulsion and attraction (neutral) activities happens is mostly observed outside and around the substituent CH_3 hydrocarbons. Similarly, the potential for ESP ranges from -2.629e-3 to 2.629e-3 as shown in Figure 7(b). From this Figure 7(b), it is observed that the effect of potential is very high around the benzene ring, while the other atoms of the substituent group experience less potential compared to the atoms near the benzene ring. Moreover, Figure 7(c) represents the electron density of the Cumene molecule showing that the molecule shows uniform structure.

Vibrational Assignments

A complete analysis of vibrational spectroscopy was carried out on the set of 57 modes. Figure 8(a) and 8(b) visualize the FT-IR and FT-Raman spectra (Ghimire et al., 2022; Khadka et al., 2023) of the Cumene molecule. The different

types of vibration across different 57 modes were observed and analysed, and these data were compared with other literatures. The two major molecular vibrations, i.e., stretching and bending, where stretching vibrations happen due to the change in bond length and bending vibrations occur due to the change in bond angle, were observed and studied. The Raman activities (Si) can be calculated by simulated equation in the Gaussian 09W software that converts the Raman activities into Raman Intensities (Ii) using the below equation derived from Raman Scattering (Sruti & Rasheed, 2015).

$$I_i = \frac{f(v_o - v_i)^4 Si}{Vi\left[1 - exp\left(\frac{-hcv_i}{kT}\right)\right]} \quad \ldots\ldots\ldots\ldots\ldots \quad (8)$$

Where v_0 is the exciting frequency (in cm^{-1} units), v_i is the vibrational wave number and h, c and k are the constant parameters and f is the common normalization factor for all peak intensities.

Figure 8

(a) FTIR Spectrum, (b) Raman Spectrum of Cumene Molecule at Neutral State

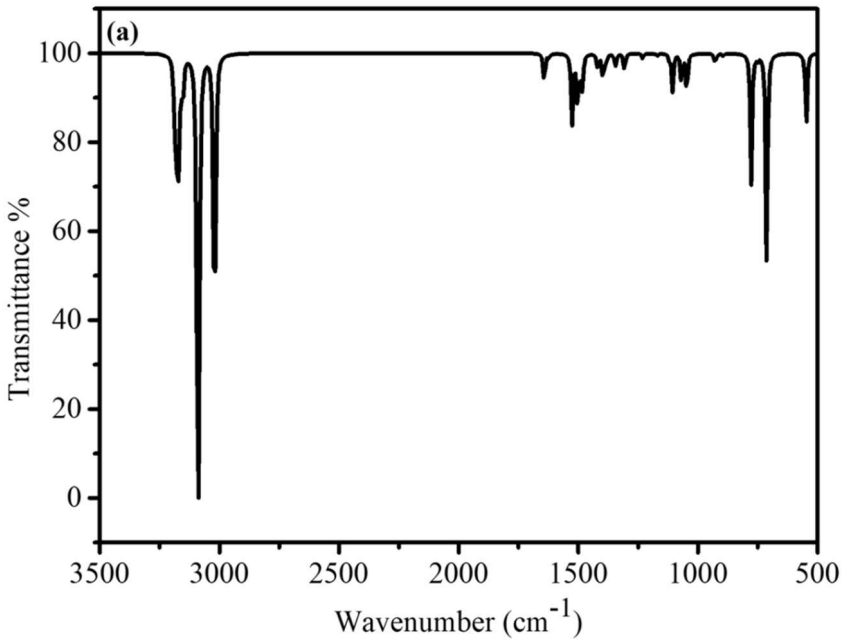

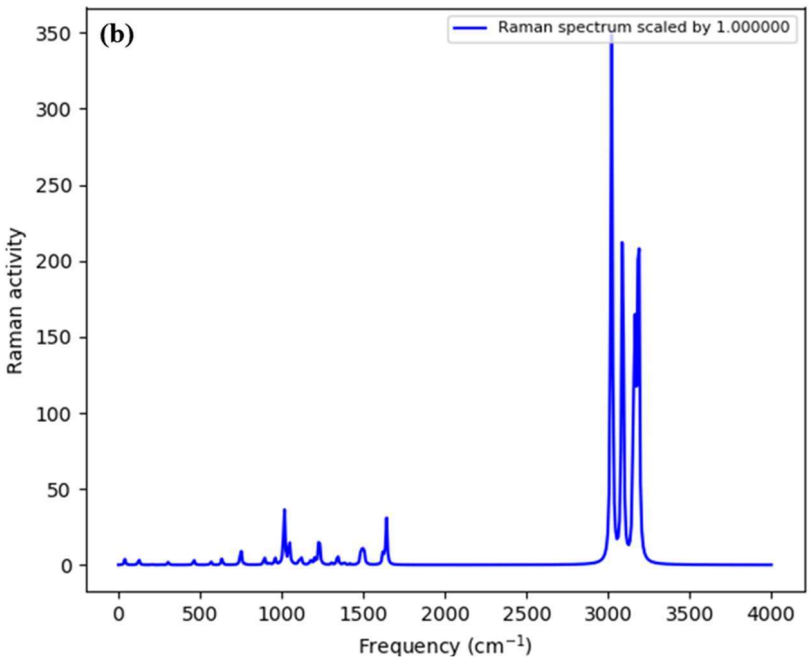

C-H Vibrations

In the case of C-H stretching vibration, it generally occurs in the region of 3100 cm^{-1} – 3000 cm^{-1} with its characteristics (Ojha et al., 2023; Pathan et al., 2023). The strong C-H stretching vibration in the Cumene molecule visualizes the frequencies at 3186 cm^{-1}, 3174 cm^{-1}, 3156 cm^{-1} and 3093 cm^{-1} in the IR spectra from Figure 8(a); while in Raman spectra from Figure 8(b), the peak vibration appears at 3018 cm^{-1} both two major stretching symmetric and antisymmetric vibrations for C-H vibrations are shown in the figure 8(a). Similarly, the in-plane bending vibration occurs normally in the mid region of 1300-1000 cm^{-1} (Arunagiri et al., 2011). The present analysis observes the frequency 1397 cm^{-1}, 1347 cm^{-1}, 1306 cm^{-1} 1105 cm^{-1} and 1046 cm^{-1} in the IR curve where the major vibration in Raman spectra is observed at 1016 cm^{-1}. The out of plane vibration is seen at the lower frequency region of 900-675 cm^{-1} (El-Saady et al., 2023b). The frequencies 777 cm^{-1}, 712 cm^{-1}, 547 cm^{-1} and 125 cm^{-1} has been assigned for out of plane vibration in the IR spectra (Figure 8(a)) where the peak vibration for Raman spectra is seen at 750 cm^{-1} (Figure 8(b)).

Methyl Group Vibrations

The symmetric and the antisymmetric stretching vibration for the CH_3 alkyl group vibrations commonly show itself at the region of 3050-2990 cm^{-1} (Mp & Seshadri, 2015). The very strong stretching vibration in the IR spectra has been observed at 3091 cm^{-1}, 3085 cm^{-1} and 3078 cm^{-1} where the most observable curve for Raman spectra has been observed at 3015 cm^{-1}. Similarly, the in-plane and out-of-plane bending vibration for CH_3 alkyl group generally occurs at mid region of 1065-1045 cm^{-1} (Nataraj et al., 2013). The current analysis shows the in-plane bending at the region of 1105 cm^{-1} , 1069 cm^{-1} and 1046 cm^{-1} in the IR spectra (Figure 8(a)) and Raman spectra show the strongest activity at 1016 cm^{-1} (Figure 8(b)). Moreover, the out-of-plane bending vibration generally occurs at the lower frequency range and has been observed at the lower region of 931 cm^{-1}, 567 cm^{-1}, 225 cm^{-1} for the IR spectra [Figure 8(a)] and 125 cm^{-1} is seen as the strongest region for Raman spectra [Figure 8(b)].

Ring Vibrations

The C=C aromatic stretching vibration usually finds its characteristics place in the region of 1625-1430 cm^{-1} (Sundaraganesan & Dominic Joshua, 2007). In the analysis of Figure 8(a), the strongest C=C stretching ring vibrations are observed at 1641 cm^{-1}, 1526 cm^{-1}, 1506 cm^{-1} and 1482 cm^{-1} in the IR spectra where the strongest observation for Raman spectra has been obtained at 1642 cm^{-1} (Figure 8(b)) and these values observed in the mentioned frequency range (Sundaraganesan & Dominic Joshua, 2007) indicate that there is no influence from the substituent part. The C-C vibrations are generally observed in the region of 1575-1430 cm^{-1} (Ojha et al., 2023). In the analysis of Figure 8(a), the C-C stretching vibrations have been observed at the region of 1386 cm^{-1}, 1343 cm^{-1}, 1306 cm^{-1} in the IR spectra.

The IR spectra of cumene in the lower region of 211-1326 cm^{-1} using the B3LYP/6-31G(d) basis set (Fishman et al., 2008) are approximately coincide with spectra found in the lower region of 125-1487 cm^{-1} in our current analysis.

Thermodynamic Parameters Analysis

The thermodynamic properties are analysed using the thermodynamic parameters and notable thermodynamic changes are seen in its structure as per the change in temperature. The Gaussian DFT B3LYP/6-311++G(d, p) basis set following the Moltran software was used to calculate the thermodynamic properties. Figure 9(a) represents the correlation graphs of heat capacity at constant volume (C_V) and heat capacity at constant pressure (C_P) with respect to temperature range in 50 K- 500 K. It shows that the C_v and C_p increase along with the increase in temperature. Figure 9(b) represents the graphs of internal energy (U) and enthalpy (H) with respect to temperature in the range 50 K - 500 K. This Figure shows that U and H also increase along with the increase in temperature starting from 50K. Figure 9(c) represents the graphs of entropy (S) and Gibb's free energy (G) with respect to temperature with the range of 50 K- 500 K. In this Figure, S also increases with increase in temperature. However, the G decreases relentlessly as it depends upon S and H of the system that shows the amount of useful work with respect to temperature where its maximum value was recorded at 50 K with the value of 481.445 kJ/mol and minimum at the maximum temperature 500 K with the value of 307.166 kJ/mol. The correlation plot of G and S shows that the two lines intersect at certain point which verifies the relation between S and G. Furthermore, the change of H and S represent that these parameters changing depend on the temperature due to which these parameters change their thermodynamic system on their own ways (Gauli et al., 2023; Seshadri & Mp, 2018).

Figure 9

Correlation Plot of Thermodynamic Parameters (a) Heat Capacity at Constant Volume and Heat Capacity at Constant Pressure, (b) Internal Energy and Enthalpy, (c) Entropy and Gibb's Free energy With Respect to Temperature

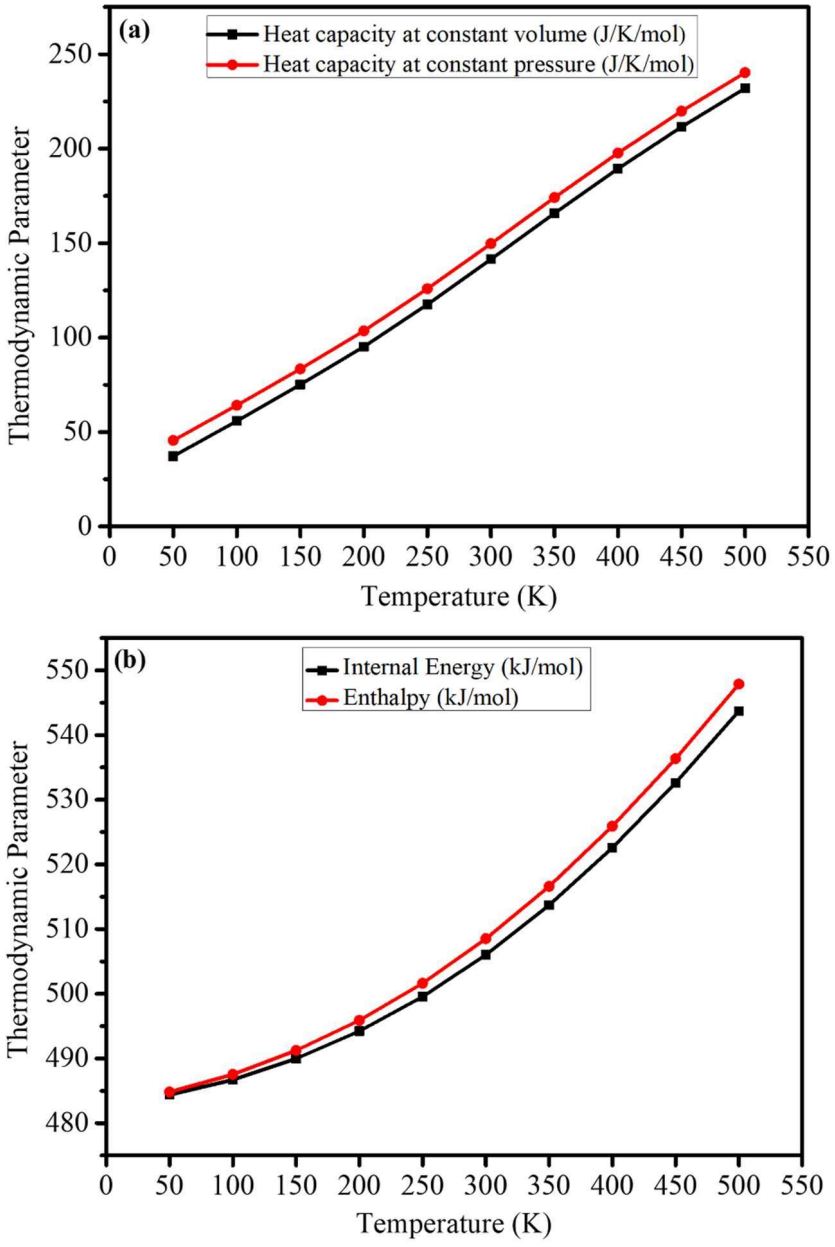

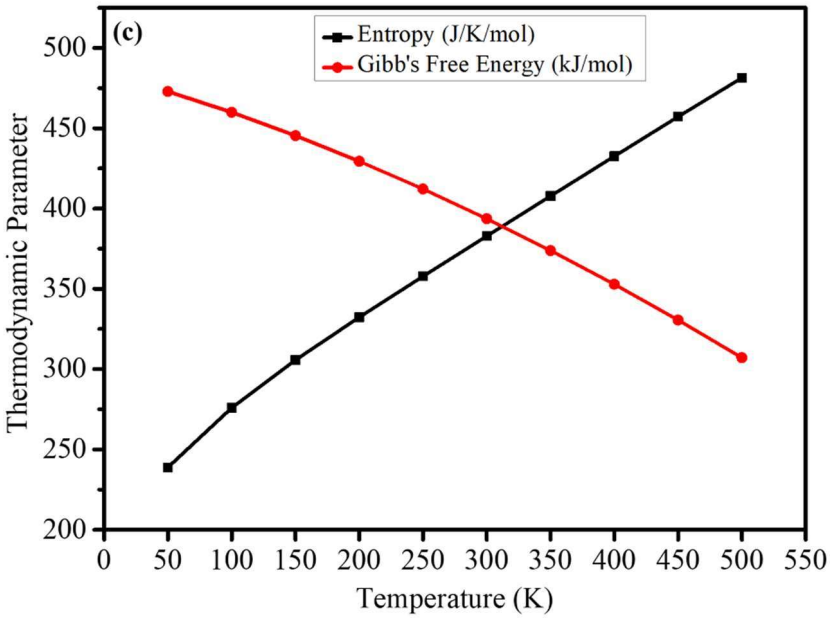

Conclusion

The first principles DFT approach with the B3LYP/6-311++G(d,p) basis set has been employed to the Cumene molecule for analysis of optimized molecular structure, electronic structure, charge analysis, FT-IR, FT-Raman spectroscopic analysis and thermodynamic properties. The optimized energy of -9531.7864 and the dipole moment of 0.3818 Debye are obtained. The bond angle, bond length and dihedral angle between the atoms inside the benzene ring and that of the substitute methyl molecule has been observed and compared with the experimental value. The HOMO-LUMO gap is observed to be 6.331eV representing the stability of the molecule and the electrophilic and nucleophilic behaviour inside the molecule which is compared with the DOS value of 6.321 eV. The global parameters such as ionization energy with 6.747 eV, electron affinity with 0.4152 eV, chemical potential with -3.5811 eV, electronegativity with 3.5811 eV, global hardness with 3.1659 eV, softness with 0.3148 eV^{-1} and electrophilicity index with 2.0253 eV have been calculated. Furthermore, the mulliken charge analysis for each atom in the molecule has been observed where

most of the C-atoms have been observed with the major negative charge and H-atoms with positive charges. The electronic structure such as MEP, ESP and ED has been studied showcasing that the area near and inside the ring structure has more electronegativity behaviour while other outside region has mild electronegativity activity. The FT-IR and FT-Raman spectroscopy identified strong C-H vibrations at 3186-3093 cm^{-1}, methyl group vibration at 3091-3078 cm^{-1} and the ring vibrations at 1641-1482 cm^{-1}. The different thermodynamic properties such as Cv, Cp, U, H, S and G are analysed with varying the temperature where the parameters such as Cv, Cp, U, H, and S increased with the rise in temperature and while the behaviour of G declines as the temperature is increased.

In overall this research analysis contributes on the field of science discovering different aromatic substance, drugs in the medical field and developing more efficient and sustainable catalysts for the Cumene related reactions for creating more environmentally friendly technological advancement in the present and future days.

References

Al-Khattaf, S., & De Lasa, H. (2001). Catalytic cracking of cumene in a riser simulator: A catalyst activity decay model. *Industrial and Engineering Chemistry Research*, *40* (23), 5398–5404. https://doi.org/10.1021/IE001141C

Arunagiri, C., Arivazhagan, M., & Subashini, A. (2011). Vibrational spectroscopic (FT-IR and FT-Raman), first-order hyperpolarizablity, HOMO, LUMO, NBO, Mulliken charges and structure determination of 2-bromo-4-chlorotoluene. *Spectrochimica Acta - Part A: Molecular and Biomolecular Spectroscopy*, *79*(5), 1747–1756. https://doi.org/10.1016/j.saa.2011.05.050

Dhakal, C. P., & Rai, K. B. (2023). Simulating and analyzing the electronic structure of a spherical amorphous SiO2 nanoparticle of finite radius. *Journal of Nepal Physical Society*, *9*(2), 14–22. https://doi.org/10.3126/jnphyssoc.v9i2.62285

Duh, Y. S. (2016). Chemical kinetics on thermal decompositions of cumene hydroperoxide in cumene studied by calorimetry: An overview. *Thermochimica Acta*, *637*, 102–109. https://doi.org/10.1016/J.TCA.2016.06.003

El-Saady, A. A., Roushdy, N., Farag, A. A. M., El-Nahass, M. M., & Abdel Basset, D. M. (2023). Exploring the molecular spectroscopic and electronic characterization of nanocrystalline Metal-free phthalocyanine: A DFT investigation. *Optical and Quantum Electronics*, *55*(7), 662. https://doi.org/10.1007/s11082-023-04877-8

Fishman, A. I., Noskov, A. I., Remizov, A. B., & Chachkov, D. V. (2008). Vibrational spectra and structure of isopropylbenzene. *Spectrochimica Acta Part A: Molecular and Biomolecular Spectroscopy*, *71*(3), 1128-1133. https://doi.org/10.1016/j.saa.2008.03.008

Gauli, H. R. K., Rai, K. B., Giri, K. & Neupane, R. (2023). Monte-carlo simulation of phase transition in 2d and 3d Ising model. *Scientific World*, *16*(16), *12-20*. doi.org/10.3126/sw.v16i16.56744

Ghimire, R. R., Dahal, Y. P. & Rai, K. B. (2023). Fabrication of UV sensing transistor based on transparent polycrystalline zinc oxide thin film using polymeric electrolyte gate dielectric. *BIBECHANA*, *20*(1), 46-54. https://doi.org/10.3126/bibechana.v20i1.51788

Ghimire, R. R., Dahal, Y. P., Rai, K. B. & Gupta, S. P. (2021). Determination of optical constants and thickness of nanostructured zno film by spin coating technique. *Journal of Nepal Physical Society*, *7*(2), 119-125. https://doi.org/10.3126/jnphyssoc.v7i2.38632

Ghimire, R. R., Parajuli, A., Gupta, S. P., & Rai, K. B. (2022). Synthesis of znO nanoparticles by chemical method and its structural and optical characterization. *BIBECHANA*, 19(1-2), 90-96. https://doi.org/10.3126/bibechana.v19i1-2.46396

Haun, J. W., & Kobe, K. A. (2002). Mononitration of cumene. *Industrial & Engineering Chemistry*, *43*(10), 2355–2362. https://doi.org/10.1021/IE50502A050

Jansang, B., Nanok, T., & Limtrakul, J. (2006). Structures and reaction mechanisms of cumene formation via benzene alkylation with propylene in a newly synthesized ITQ-24 zeolite: An embedded ONIOM study. *Journal of Physical Chemistry B*, *110*(25), 12626–12631. https://doi.org/10.1021/jp061644h

Kaya, S., & Kaya, C. (2015). A new method for calculation of molecular hardness: A theoretical study. *Computational and Theoretical Chemistry*, *1060*, 66–70. https://doi.org/10.1016/J.COMPTC.2015.03.004

Khadka, I. B., Rai, K. B., Alsardia, M. M., Haq, B. U. & Kim, S. H. (2023). Raman investigation of substrate-induced strain in epitaxially grown

graphene on low/high miscut angled silicon carbide and its application perspectives. *Optical Materials*, *140*, 113836. doi.org/10.1016/j.optmat.2023.113836

Kumer, A., Sarker, M. N., & Paul, S. (2019). The theoretical investigation of HOMO, LUMO, thermophysical properties and QSAR study of some aromatic carboxylic acids using HyperChem programming. *International Journal of Chemistry and Technology*, *3*(1), 26–37. https://doi.org/10.32571/ijct.478179

Limbu, S., Ojha, Ghimire, R. R. & Rai K. B. (2024). An investigation of vibrational analysis, thermodynamics properties and electronic properties of Formaldehyde and its stretch by substituent acetone, acetyl chloride and methyl acetate using first principles analysis. *BIBECHANA*, *21*(1), 23–36. https://doi.org/10.3126/bibechana.v21i1.58684

Luyben, W. L. (2010). Design and Control of the Cumene Process. *Industrial & Engineering Chemistry Research, 49*(2), *719–734*. https://doi.org/10.1021/ie9011535

Mp, R., & Seshadri, S. (2015). Quantum mechanical Study of the structure and spectroscopic (FTIR, FT-Raman, NMR and UV), first order hyperpolarizability and HOMO-LUMO analysis of 2-[(Methylamino) Methyl] pyridine. *Article in IOSR Journal of Applied Physics*, *7*(6), 56–70. https://doi.org/10.9790/4861-07615670

Nataraj, A., Balachandran, V., & Karthick, T. (2013). Molecular structure, vibrational spectra, first hyperpolarizability and HOMO–LUMO analysis of p-acetylbenzonitrile using quantum chemical calculation. *Journal of Molecular Structure*, *1038*, 134-144. https://doi.org/10.1016/j.molstruc.2013.01.054

Nikfar, S., & Behboudi, A. F. (2014). Cumene. *Encyclopedia of toxicology: Third edition*, 1082–1085. https://doi.org/10.1016/B978-0-12-386454-3.00599-6

Ojha, J. K., Ramesh, G., & Reddy, B. V. (2023). Structure, chemical reactivity, NBO, MEP analysis and thermodynamic parameters of pentamethyl benzene using DFT study. *Chemical Physics Impact*, *7,* 2667-0224. https://doi.org/10.1016/j.chphi.2023.100280

Ojha, T., Limbu, S., Shrestha, P. M., Gupta, S. P. & Rai, K. B. (2023). Comparative computational study on molecular structure, electronic and vibrational analysis of vinyl bromide based on HF and DFT approach. *Himalayan Journal of Science and Technology*. *7*(1), 38- 49. https://doi.org/10.3126/hijost.v7i1.61128

Pathan, H. K., Khanum, G., Javed, R., Siddiqui, N., Selvakumari, S., Muthu, S., Ali, A., Arora, H., Afzal, M., Kumar, A. & Javed, S. (2023). Quantum computational, spectroscopic characterization, Hirshfeld analysis & molecular docking studies on p-toluenesulfonic acid (p-TSA) or tosylic acid. *Chemical Physics Impact*, *7*, 100320. https://doi.org/10.1016/j.chphi.2023.100320

Petroselli, M., Melone, L., Cametti, M., & Punta, C. (2017). Lipophilic N-hydroxyphthalimide catalysts for the aerobic oxidation of cumene: Towards solvent-free conditions and back. *Chemistry – A European Journal*, *23*(44), 10616–10625. https://doi.org/10.1002/CHEM.201701573

Prabhu, C., Rajesh, P., Dhanalakshmi, E., Gnanasambandan, T. & Priyadharshini, M. (2023). Structure conformational, molecular docking and computational investigation of methyl linoleate. *Chemical Physics Impact*, *7*, 100300. https://doi.org/10.1016/j.chphi.2023.100300

Rai, K. B., Ghimire, R. R., Dhakal, C., Pudasainee, K. & Siwakoti, B. (2024). Structural equilibrium configuration of benzene and aniline: A first-principles study. *Journal of Nepal Chemical Society*. *44*(1), 1-15. https://doi.org/10.3126/jncs.v44i1.62675

Seshadri, S., & Mp, R. (2018). Structural, spectroscopic characterization and docking study of 4-amino-3-nitropyridine with experimental technique and quantum chemical calculations. *International Journal of Creative Research Thoughts, 6*(1), 43-61. https://doi.org/10.13140/RG.2.2.10527.25761

Sivaranjani, T., Xavier, S., & Periandy, S. (2015). NMR, FT-IR, FT-Raman, UV spectroscopic, HOMO-LUMO and NBO analysis of Cumene by quantum computational methods. *Journal of Molecular Structure*, *1083*, 39–47. https://doi.org/10.1016/j.molstruc.2014.11.035

Sruti, S., & Rasheed, M. P. (2015). Vibrational spectroscopic (FTIR and FT-Raman) studies, HOMO LUMO analysis, NMR chemical shifts and electrostatic potential surface of 2, 3-dibromofuran. *Frontiers in Optics, 18-22*. https://doi.org/10.1364/fio.2015.jw2a.23

Sundaraganesan, N., & Dominic Joshua, B. (2007). Vibrational spectra and fundamental structural assignments from HF and DFT calculations of methyl benzoate. *Spectrochimica Acta - Part A: Molecular and Biomolecular Spectroscopy*, *68*(3), 771–777. https://doi.org/10.1016/j.saa.2006.12.059

Torrent-Sucarrat, M., Duran, M., & Sola, M. (2002). Global hardness evaluation using simplified models for the hardness kernel. *The Journal of Physical Chemistry A, 106(18), 4632–4638.* https://doi.org/10.1021/jp013249r

Vinodkumar, R., Jayavarthanan, T., Suresh, S., Periandy, S., & Venkatachalapathy, V. S. K. (2023). Spectroscopic (FTIR, FT-Raman, UV–Vis) studies, NMR, NBO analysis, molecular docking studies on 2-cyano-5-fluoropyridine and 3-cyano-2-fluoropyridine. *Chemical Physics Impact*, *7*, 2667-0224. https://doi.org/10.1016/j.chphi.2023.100378

Weast, R. C. (1975). *CRC Handbook of chemistry and physics: A ready Reference book of chemical and physical data*, 76th edition, CRC Press, USA.A peer-reviewed open-access journal indexed in NepJol